IV International Conference on Computational Methods for Coupled Problems in Science and Engineering
COUPLED PROBLEMS 2011
M. Papadrakakis, E. Oñate and B. Schrefler (Eds)

NUMERICAL SIMULATION OF AILERON BUZZ USING AN ADAPTIVE-GRID COMPRESSIBLE FLOW SOLVER FOR DYNAMIC MESHES

Giuseppe Forestieri, Alberto Guardone, Dario Isola, Filippo Marulli and Giuseppe Quaranta

Dipartimento di Ingegneria Aerospaziale,
Politecnico di Milano,
Via La Masa 34, 20156, Milano, Italy.
e-mail: alberto.guardone@polimi.it, www.aero.polimi.it/flowmesh

Key words: Arbitrary Lagrangian Eulerian, Adaptive mesh, Fluid Structure Interaction, Aileron Buzz

Abstract. The paper presents numerical results from a novel scheme for the solution of the flow equations in two dimensional domains by an Arbitrary Lagrangian Eulerian formulation able to cope with deforming and adaptive two dimensional grids without recurring to any explicit interpolation scheme. The method is applied to the investigation of a classical transonic aeroelastic instability phenomenon: the aileron buzz. By resorting to deforming and adaptive grids, the method allows to highlight the dependency of the aeroelastic stability boundaries on the mesh spacing.

1 INTRODUCTION

The investigation of aeroelastic stability boundaries by means of Fluid Structure Interaction (FSI) analysis is becoming very popular for the preliminary and verification phases of new aircraft design [2, 14], and it is currently denominated Computational Aeroelasticity (CA). By resorting to CFD models based on Euler or Reynolds-Averaged Navier-Stokes (RANS) equations, these approaches avoid any unduly simplification in the computation of fluid flow unsteady forces, allowing to keep into account also the effect of shock-waves, and flow separations, usually neglected by classical potential approaches.

To obtain reliable results, appropriate meshes of the fluid domain must be used. What should be a reliable mesh for a static fluid flow simulation around an aircraft could be considered a question that received an answer in the literature. The same cannot be said if unsteady flow simulations in transonic flow fields are considered, as those that are of paramount importance for CA cases. The paper investigates the dependency of the stability boundary from the grid spacing showing how simulation based on time-

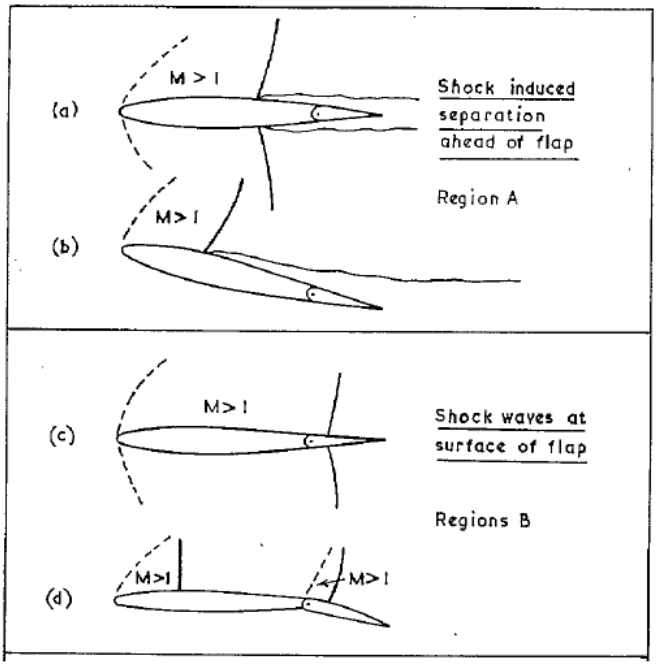

Figure 1: Aerodynamic conditions for which buzz may occur; taken from Ref. [11].

adaptive mesh may improve significantly the prediction capability of numerical approaches to aeroelasticity.

In the present work it has been decided to start tackling this problem by analyzing the dependency from the grid of the numerically evaluated stability boundary of a simple transonic aeroelastic problem characterized by a single structural degrees of freedom: the aileron buzz. This is an instability involving the interaction of a single structural degree of freedom, associated to the aileron rotation about its hinge, with unsteady aerodynamic forces caused by strong shock waves dwelling close to the hinge axis. The instability may evolve into self-sustained Limit Cycle Oscillations [10, 11]. Two principal classes of buzz have been shown during experimental campaigns. Following the classification proposed by Lambourne [10] (see figure 1), the Type A is caused by interaction of the shock-waves with the boundary layer, while Type B results from to the interaction of the shock-waves with the aileron movement without significant intervention of the boundary layer. This latter case is commonly denominated non-classical. Type A is characterized by shock waves positioned ahead of the hinge line, while for Type B phenomena the shock waves are at the flap surface, so they appear at higher Mach numbers than Type A. If a numerical approach is adopted to study the buzz problem, the Euler equations can be considered a good description of the fluid behaviour only for the Type B phenomena since no interaction with the boundary layer is necessary to capture the unsteady forces. Consequently, this paper investigates the Type B buzz taking as a reference the experimental work done

by Lambourne [10]. For numerical analysis of Type A phenomena see [3] and references therein.

The simulation of the buzz phenomenon requires one to perform unsteady simulations of the flowfield while the computational domain is continuously changing its shape to account for the flap movement. So Arbitrary Lagrangian Eulerian (ALE) formulation joined with appropriate mesh update scheme must be considered. The innovative two-dimensional numerical scheme for the compressible CFD equations on dynamic meshes proposed in [9, 13] has been used. It allows to perform computations on moving meshes with adaptation, which is required to preserve the mesh spacing for large boundary displacement.

The paper is organized as follow. The second section briefly presents the numerical approach used for the analysis of fluid flow equations with movable and adaptive grids. The third section shows the detail of the FSI models together with the partitioned strategy used to integrates the two-domain problem. Finally, the numerical results section shows the result obtained with different grids with variable refinement levels, and those obtained by using the adaptive approach.

2 FINITE VOLUME ALE SCHEME

The governing equations for a compressible inviscid fluid in two spatial dimensions are provided by the well-known Euler equations in an Arbitrary Lagrangian Eulerian (ALE) framework [6], namely,

$$\frac{d}{dt}\int_{\mathcal{C}(t)} \mathsf{u} + \oint_{\partial\mathcal{C}(t)} \left[\mathbf{f}(\mathsf{u}) - \mathsf{u}\,\boldsymbol{v}\right]\cdot\boldsymbol{n} = 0, \qquad \forall \mathcal{C}(t) \subseteq \Omega(t), \tag{1}$$

completed by suitable initial and boundary conditions [8]. In Eq. (1) $\mathsf{u} = (\rho, \boldsymbol{m}, E^{\mathrm{t}})^{\mathrm{T}}$, is the vector unknown of the density ρ, momentum vector $\boldsymbol{m}$, and total energy per unit volume E^{t} and the flux function is defined as

$$\mathbf{f}(\mathsf{u}) = \left(\boldsymbol{m},\ \boldsymbol{m}\otimes\boldsymbol{m}/\rho + P(\mathsf{u})\ \mathsf{I},\ \left[E^{\mathrm{t}} + P(\mathsf{u})\right]\boldsymbol{m}/\rho\right)^{\mathrm{T}}$$

where I is the 2×2 identity matrix and P is the pressure. The term $\mathsf{u}(\boldsymbol{v}\cdot\boldsymbol{n})$ takes into account the flux contribution due to the movement of the boundary of the control volume $\partial\mathcal{C}(t)$ with normal vector $\boldsymbol{n}(t)$.

A standard node-centered finite volume scheme is used to discretize the governing equation. [9] As shown in figure 2, a non overlapping set of cells $\mathcal{C}_i$ is taken to discretize Ω and the unknown u is approximated over $\mathcal{C}_i$ by its average value $\mathsf{u}_i = \mathsf{u}_i(t)$. Eq. (1) can be rewritten

$$\frac{d}{dt}\left[V_i\,\mathsf{u}_i\right] = \sum_{k\in\mathcal{K}_{i,\neq}} \Phi_{ik}(\mathsf{u}_i, \mathsf{u}_k, \nu_{ik}, \boldsymbol{\eta}_{ik}) + \Phi_i^{\partial}(\mathsf{u}_i, \nu_i, \boldsymbol{\xi}_i) \qquad \forall i \in \mathcal{K} \tag{2}$$

where Φ_{ik} and Φ_i^{∂} are the domain and boundary numerical fluxes, $\mathcal{K}_{i,\neq}$ is the set of nodes connected to i by an edge, $\boldsymbol{\eta}_{ik}$ and $\boldsymbol{\xi}_i$ are the normal vectors integrated along the interface

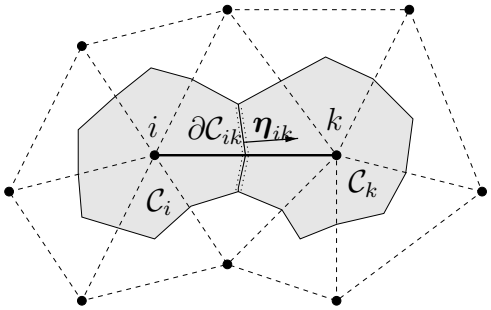

Figure 2: Edge associated with the finite volume interface $\partial\mathcal{C}_{ik} = \partial\mathcal{C}_i \cap \partial\mathcal{C}_k$ and metric vector $\boldsymbol{\eta}_{ik}$ (integrated normal) in two spatial dimensions. The two shaded regions are the finite volumes $\mathcal{C}_i$ and $\mathcal{C}_k$; dashed lines indicate the underlying triangulation.

and ν_{ik} and ν_i are the integrated normal velocities. A high-resolution expression for the integrated numerical flux [15] is used in the present work based on the Total Variation Diminishing (TVD) approach.

In order to ensure the conservativity of the scheme the well known Geometric Conservation Law [5] has to be satisfied. This is often achieved by choosing the integrated interface velocities as the time derivative of the volume swept by the interface, namely

$$\frac{dV_{i,ik}}{dt} = \int_{\partial\mathcal{C}_{ik}} \boldsymbol{v}\cdot\boldsymbol{n} \qquad \text{and} \qquad \frac{dV_{i,\partial}}{dt} = \int_{\partial\mathcal{C}_i\cap\partial\Omega} \boldsymbol{v}\cdot\boldsymbol{n}. \tag{3}$$

Eq. (2) is solved for the fluid variables u at time level $n+1$ implicitly by means of standard integration techniques. The Jacobian matrix is computed by resorting to a first order approximation of the integrated fluxes and a dual time-stepping technique [16]. Second and third order Backward Differentiation Formula (BDF) schemes are adopted to approximate the time derivatives.

Following [12] and [9] the numerical scheme outline above is used together with mesh adaptation techniques. The local modifications of the topology of the grid occurring during the adaptation step, e.g. edge-swapping and node insertion/deletion, are interpreted as a continuous deformation of the finite volumes associated to the grid. The interface velocities given by Eq. (3) are thus computed accounting for the distortion of the finite volumes caused by the modifications in grid topology. Such approach allows to compute the solution onto the new, adapted, grid simply integrating Eq. (2) without any explicit interpolation step. To ensure the conservativity of the resulting scheme additional flux contributions must be taken into account for every removed edge [12] and additional conservation equations must be integrated for every removed node [9]. Such additional fluxes and equations can be dropped after a given number of time steps depending on the time-integration scheme adopted, e.g. two for a BDF2 and three a BDF3, since their contribution is identically equal to zero.

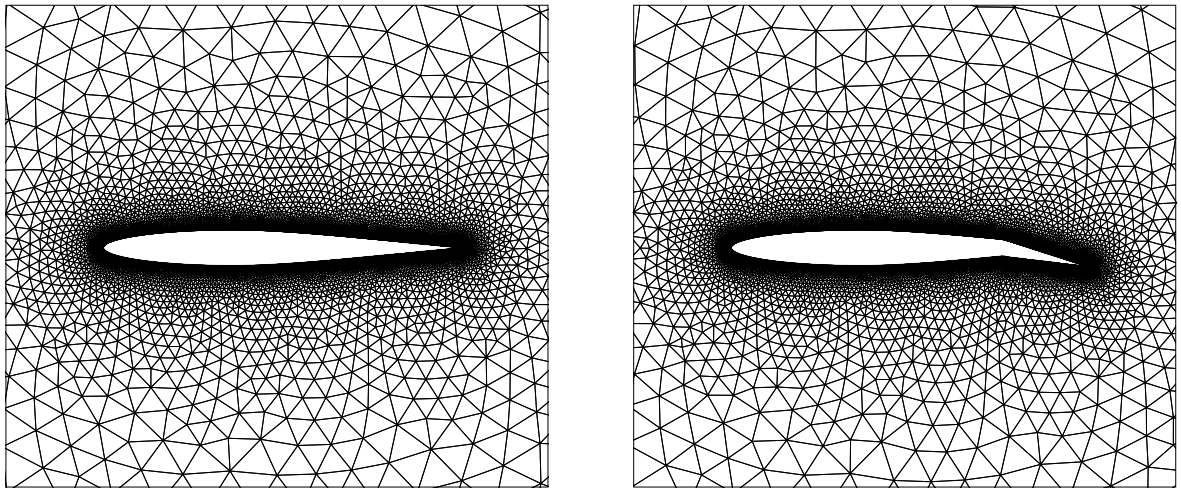

(a) $\beta = 0°$ (b) $\beta = 12°$

Figure 3: Numerical grid for two flap rotations.

3 FLUID-STRUCTURE INTERACTION MODELING FOR THE AILERON BUZZ

The structural model used to describe the aileron motion is a simple one degree of freedom equation expressing equilibrium of moments about the aileron hinge, namely

$$I\ddot{\beta} = M \ , \tag{4}$$

where I is the inertia moment of the flap around the hinge and M is the aerodynamic moment about the hinge line. Given the value of the flap rotation β at a given time t^{n+1}, the position of the grid nodes belonging to the boundary is updated and the inner nodes are displaced resorting to a mesh deformation algorithm based on the elastic analogy that preserves the good quality of elements close to the airfoil [12, 4].

The direct time integration of the fluid-structure interaction problem is tackled using a partitioned loosely coupled algorithm. Both aerodynamic and structural systems are integrated using an implicit scheme, thus achieving linear stability for any value of time-step Δt. In particular, Eq. 2 has been integrated using a second order accurate BDF scheme, while a predictor-corrector method derived from Crank-Nicholson [7] has been adopted for the structural subsystem. The latter scheme is here briefly outlined.

1. The known values of flap angle, flap angular velocity and aerodynamic loads at the time n are used to prediction of the structural state at time $n+1$, i.e.

$$\begin{cases} \beta_p^{n+1} = \beta^n + \Delta t\, \dot{\beta}^n + \frac{\Delta t^2}{2I} M^n, \\ \dot{\beta}_p^{n+1} = \dot{\beta}^n + \frac{\Delta t}{I} M^n. \end{cases}$$

2. The predicted predicted structural state, β_p^{n+1} and $\dot{\beta}_p^{n+1}$ is used to compute the new mesh and subsequently the aerodynamic loads, $M^{n+1} = M(\beta_p^{n+1}, \dot{\beta}_p^{n+1})$.

3. The predicted loads are used to correct the value of the structural state at t^{n+1}, i.e.

$$\begin{cases} \beta^{n+1} = \beta^n + \Delta t\, \dot{\beta}^n + \frac{\Delta t^2}{2I} \frac{M^{n+1}+M^n}{2}, \\ \dot{\beta}^{n+1} = \dot{\beta}^n + \frac{\Delta t}{I} \frac{M^{n+1}+M^n}{2}. \end{cases}$$

4 NUMERICAL RESULTS

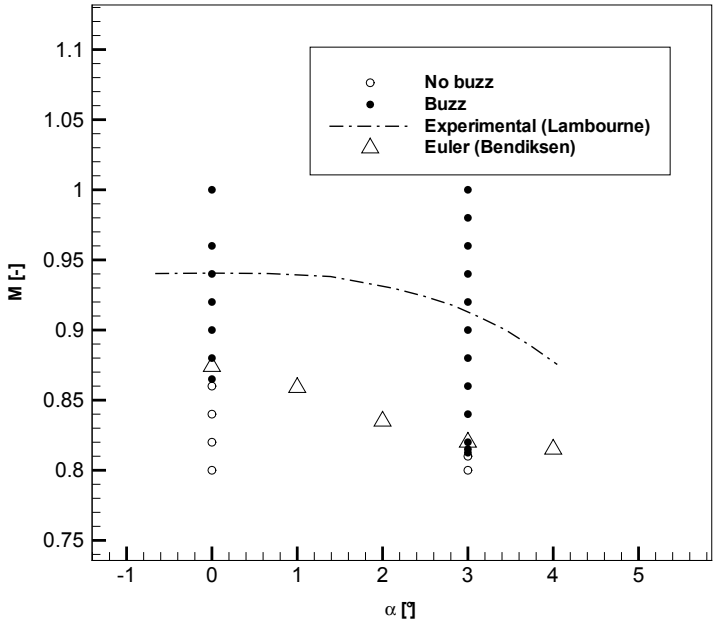

Figure 4: Comparison of experimental and numerical stability boundaries of the Mach-angle-of attack plane.

Aileron buzz is now examined to study the suitability of the proposed approach to investigate aeroelastic phenomena in two dimensional cases. The prerogative is to assess non-classical aileron buzz (type B using Lambourne classification [10]) over a range of transonic Mach numbers. Tests are conducted on a RAE 102 typical section model clamped on its mass center to avoid pitch or plunge movements and to allow only flap rotation around its hinge. Flap-chord/chord ratio is 25% and non-dimensional frequency parameter is $f = 0.063$ approximately (which corresponds to a reduced frequency of $k = \omega c/V_\infty = 0.1$). A circular domain with a radius of 20 chords is chosen to avoid

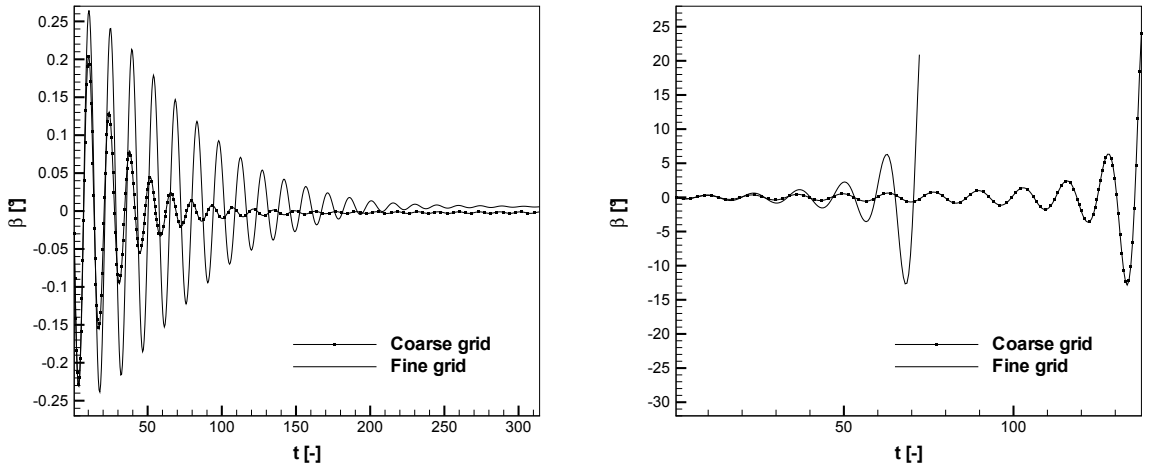

(a) M=0.86375 (b) M=0.865

Figure 5: Comparison of flap rotation transient at $\alpha = 0°$ on different grids : (a) stable responses; (b) unstable responses.

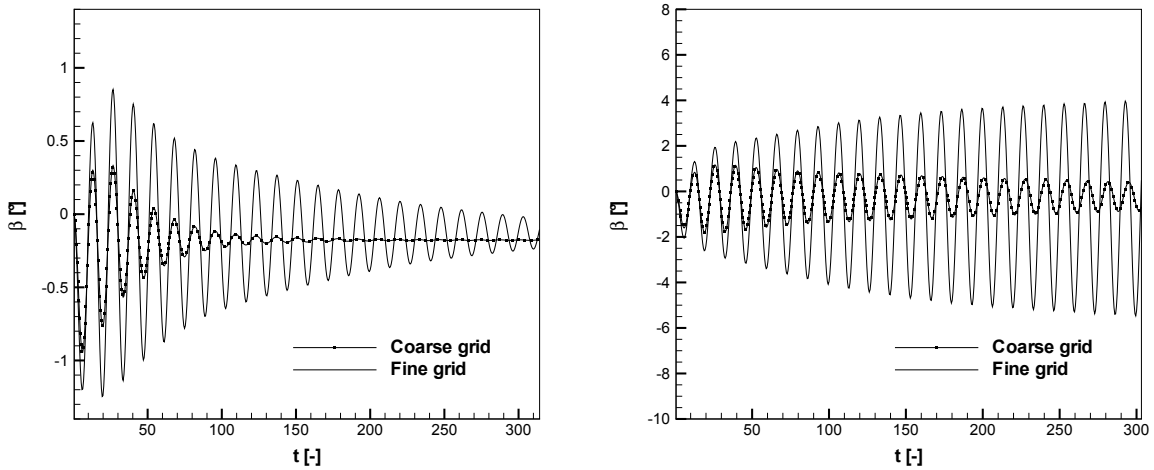

(a) M=0.81 (b) M=0.8125

Figure 6: Comparison of flap rotation transient at $\alpha = 3°$ on different grids : (a) stable response; (b) unstable/stable responses.

far-field boundary conditions interferences on the unsteady phenomenon. The result obtained is the stability boundary in the Mach-angle-of-attack plane. Since RAE 102 is a symmetrical airfoil, tests at $\alpha = 0°$ are conducted imposing a non-dimensional initial

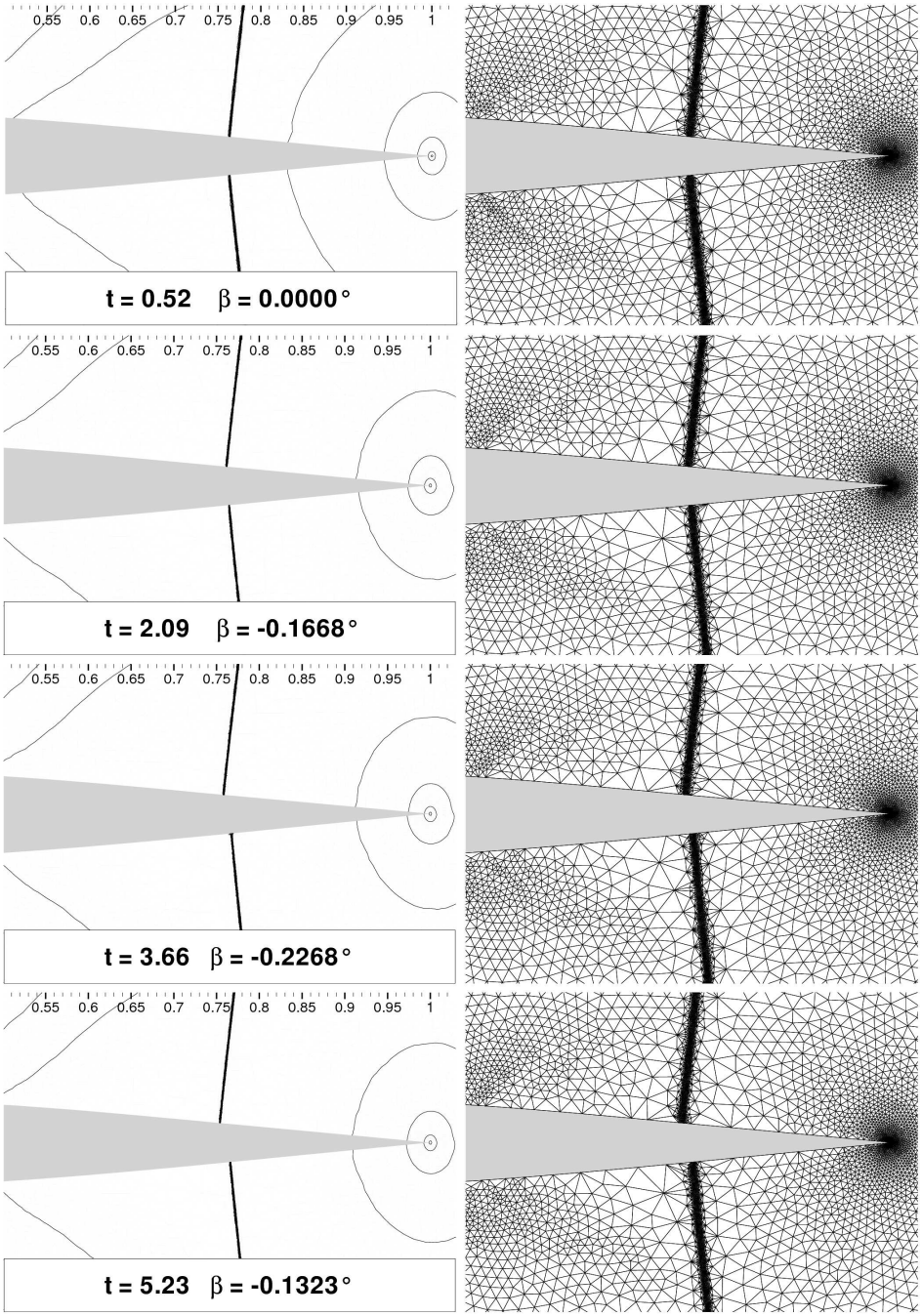

Figure 7: Snapshots of adapted grids and Mach number contour during a cycle of an unstable aileron buzz case (M=0.865,$\alpha = 0°$).

angular velocity of flap around the hinge different from zero ($\dot{\beta} = -10^{-3}$). Differently, computations with an angle of attack $\alpha = 3°$ don't need an initial perturbation thank to

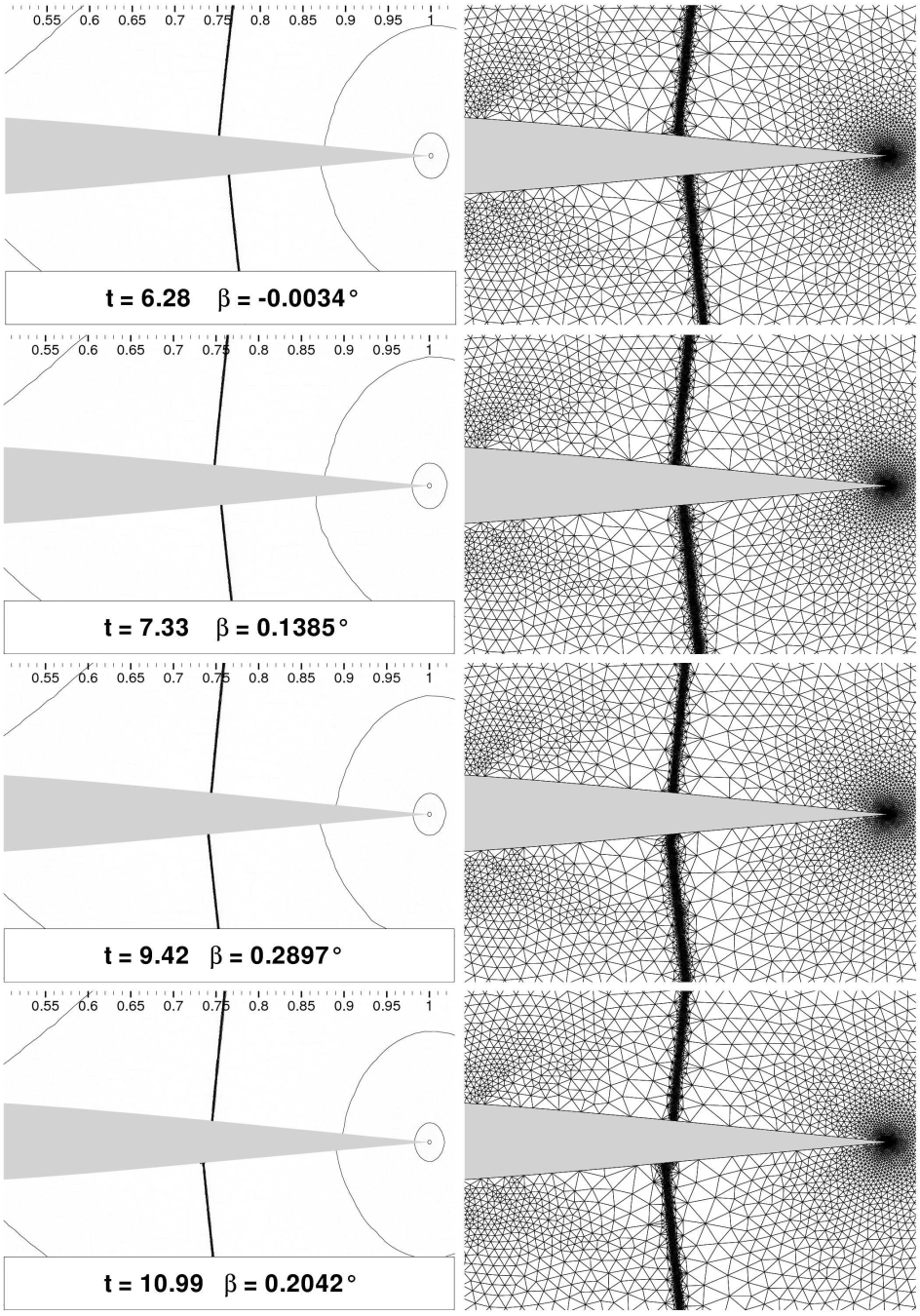

Figure 8: Snapshots of adapted grids and Mach number contour during a cycle of an unstable aileron buzz case (M=0.865,$\alpha = 0°$).

a sufficient initial value of flap hinge moment coefficient $C_m = \frac{M}{1/2\rho V^2 c^2}$.

Numerical computations are conducted at different Mach numbers ($0.8 < M < 1.0$) with two different angles of attack ($\alpha = 0°, \alpha = 3°$) in order to define numerical boundary stability. Moreover two different grids are used to perform a sensitivity of the phenomenon with respect to the computational discretization spacing; a coarse grid with 10 396 nodes and 19 745 elements and a fine computational grid with 20 845 nodes and 40 482 elements. All computations are performed using the second-order BDF time integration scheme with $\Delta t = 0.5235$ and a non-dimensional simulation time $T = 314.15$.

Figure 4 shows the comparison of the computed stability boundary on the Mach-angle-of-attack plane with the experimental one. Euler equations model produces a result far away from the experimental model instability [10]. In fact, since viscous effects are not considered in Euler equations, a lower stability boundary is obtained. Boundary layer presence implies an increase airfoil thickness for inviscid flow providing an higher stability boundary in terms of Mach number. On the other hand, numerical results are in fairly good agreement with inviscid computations by Bendiksen [1].

In figure 5 is shown the response in terms of flap rotation β for $\alpha = 0°$ across the stability boundary (respectively M=0.86375 and M=0.865) using two different grid spacings. In general, a reduced grid spacing determines a more negative aerodynamic damping effect, both for stable and unstable cases. This is due to numerical viscosity increase with volume cell. Flap rotation responses for $\alpha = 3°$ are shown in figure 6. In this case numerical stability boundary has been evaluated about M=0.8125. In fact, across this value of Mach number a different behaviour can be noticed in changing grid space. The fine grid gives an unstable response while the coarse grid a stable one. This is in agreement with the increase of aerodynamic damping effect with cell volume.

Figure 7 and figure 8 show the details of some subsequent flow-fields around the flap during an unstable response at $M = 0.865$, $a = 0°$. Numerical computation has been performed using a *grid adaptation* technique to improve the capturing of shocks movements on airfoil and flap surface. Mesh adaptation has been driven by an error indicator based on the Hessian matrix and the gradient of the Mach number over the whole computation domain. Initial grid at $t = 0^-$ has been created using 21 625 nodes and 42 747 elements. When the flap starts moving upward the upper shock moves forward and lower its strength while the lower shock does the opposite.

5 CONCLUSIONS

A novel conservative adaptive-grid for the Euler equations was applied to the computation of the stability boundary for the non-classical buzz problem for the RAE 102 airfoil. The proposed technique does not require cross-grid reinterpolation. As expected, for a given angle of attack, numerical simulations of the buzz phenomena on the denser grid are found to indicate a lower stability limit for the Mach number with respect to coarse grid computations. Remarkably enough, adapted grid computations are found to be less accurate in predicting the location of the stability boundary with respect to the coarse and dense grid ones, which is higher for the adapted case. This is believed to be related

to the adaptation sensors, which allows to gather grid points close to the shock wave but it is not sufficient to increase the accuracy in the smooth regions that contribute to the overall value of the hinge momentum. Current research activities are devoted to further study suitable sensors to improve the adaptation process in terms of the evaluation of the stability limit.

REFERENCES

[1] O.O. Bendiksen. Nonclassical aileron buzz in transonic flow. *34th AIAA/ASME/ASCE/AHS/ASC Structures, Structural Dynamics and Materials Conference*, pages (AIAA Paper 93–1479), April 1993.

[2] Robert M. Bennet and John W. Edwards. An overview of recent developments in computational aeroelasticity. In *Proceedings of the* 29th *AIAA Fluid Dynamics Conference*, Albuquerque, NM, June 15-18 1998.

[3] Edoardo Biganzoli and Giuseppe Quaranta. Nonlinear reduced order models for aileron buzz. In *International Forum on Aeroelasticity and Structural Dynamics (IFASD 2009)*, Seattle, WA, USA, 21–25 June 2009.

[4] Luca Cavagna, Giuseppe Quaranta, and Paolo Mantegazza. Application of Navier-Stokes simulations for aeroelastic assessment in transonic regime. *Computers & Structures*, 85(11-14):818–832, 2007.

[5] J. Donea. A Taylor–Galerkin method for convective transport problems. *Int. J. Numer. Meth. Eng.*, 20:101–119, 1984.

[6] J. Donea, A. Huerta, J.-Ph. Ponthot, and A. Rodríguez-Ferran. Arbitrary lagrangian-Eulerian methods. In R. Stein, E. de Borst, and T.J.R. Hughes, editors, *The Encyclopedia of Computational Mechanics*, volume 1, chapter 14, pages 413–437. Wiley, 2004.

[7] M. B. Giles. Stability analysis of a Galerkin/runge–Kutta navier–stokes discretization on unstructured tetrahedral grids. *J. Comput. Phys.*, 132:201–214, 1997.

[8] E. Godlewski and P. A. Raviart. *Numerical approximation of hyperbolic systems of conservation laws*. Springer-Verlag, New York, 1994.

[9] Dario Isola, Alberto Guardone, and Giuseppe Quaranta. An ALE scheme without interpolation for moving domain with adaptive grids. In *AIAA 40th Fluid Dynamics Conference and Exhibit*, Chicago, IL, USA, 28 June–1 July 2010.

[10] N.C. Lambourne. Flutter in one degree of freedom. In *Manual on Aeroelasticity, Part V*, chapter 5. AGARD, 1961.

[11] N.C. Lambourne. Control–surface buzz. Reports and Memoranda 3364, Aeronautical Research Council, London, UK, May 1964.

[12] D. Muffo, G. Quaranta, and A. Guardone. Compressilbe fluid-flow ale formulation on changing topology meshes for aeroelastic simulations. In *Proceedings of the* 26$^{\text{th}}$ *ICAS Congress*, Anchorage, Alaska, September 14–19 2008.

[13] Giuseppe Quaranta, Dario Isola, and Alberto Guardone. Numerical simulation of the opening of aerodynamic control surfaces with two-dimensional unstructured adaptive meshes. In *5th European Conference on Computational Fluid Dynamics - ECCOMAS CFD 2010*, Lisbon, Portugal, 14–17 June 2010.

[14] David M. Schuster, D. D. Liu, and Lawrence J. Huttsell. Computational aeroelasticity: Success, progress, challenge. *Journal of Aircraft*, 40(5):843–856, 2003.

[15] B. van Leer. Towards the ultimate conservative difference scheme II. Monotoniticy and conservation combined in a second order scheme. *J. Comput. Phys.*, 14:361–370, 1974.

[16] V. Venkatakrishnan and D. J. Mavriplis. Implicit method for the computation of unsteady flows on unstructured grids. *J. Comput. Phys.*, 127:380–397, 1996.